

# Micro-LEDs and Quantum based-Full Color Devices for Display and Visible Light Communications

**Hao-Chung Kuo<sup>1,2,\*</sup>, Wei-Ta Huang<sup>1,2</sup>, Konthoujam James Singh<sup>1</sup>, Chi-Wai Chow<sup>1</sup>, Gong-Ru Lin<sup>3</sup> and Shih-Chen Chen<sup>2</sup>**

<sup>1</sup>Department of Photonics, College of Electrical and Computer Engineering, National Yang Ming Chiao Tung University, Hsinchu 30010, Taiwan

<sup>2</sup>Semiconductor Research Center, Hon Hai Research Institute, Taipei 11492, Taiwan

<sup>3</sup>Department of Electrical Engineering, Graduate Institute of Photonics and Optoelectronics, and National Taiwan University (NTU), Taipei 10617, Taiwan

Author e-mail address: [hckuo0206@nycu.edu.tw](mailto:hckuo0206@nycu.edu.tw)

**Abstract:** Red-green-blue (RGB) full-color micro light-emitting diodes ( $\mu$ -LEDs) fabricated from semipolar (20-21) wafers, with a quantum-dot photoresist color-conversion layer, were demonstrated. We also demonstrated high-stability quantum dot-converted 3-in-1 full-color mini-light-emitting diodes passivated with low-temperature atomic layer deposition. A hybrid QD-NR- $\mu$ LED with an ALD passivation layer and efficient NRET has been fabricated to produce a monolithic RGB  $\mu$ LED device with QDs printed by super-inkjet (SIJ) printing system. We also presented a high-efficiency InGaN red micro-LED fabricated by the incorporation of superlattice structure, atomic layer deposition passivation, and a distributed Bragg reflector. Finally, a high 3-dB bandwidth semipolar (20–21) long-wavelength InGaN/GaN  $\mu$ LED has been demonstrated.

## 1. Introduction

Owing to many performance advantages over common-use technologies, micro light emitting diodes ( $\mu$ -LEDs) are the promising candidate for next generation display technology [1-4]. Red-green-blue (RGB)  $\mu$ -LEDs can be assembled to achieve full color displays using mass transfer process; however, there are still some challenges in terms of low transfer yield, slow throughput and high manufacturing cost [5]. To overcome these challenges, color conversion based on quantum dots (QDs) which requires a blue or UV-LEDs as pumping source is adopted but commercial UV-LEDs are grown on c-plane sapphire substrate. In recent years, micro-LEDs have received considerable attention for applications in next-generation displays and visible light communication (VLC) due to their fast response, light weight, low power consumption, high brightness, and high efficiency [6, 7]. GaN based LEDs grown on c-plane substrates suffer from efficiency droop caused by quantum confined Stark Effect (QCSE) resulting from polarization related electric field [8, 9]. GaN is a hexagonal crystal with a structure of wurtzite symmetry, the highest structure consistent with spontaneous piezoelectric polarization. Owing to spontaneous and piezoelectric polarization, as c -plane- grown GaN materials are subject to high built-in electric fields. LEDs based on c-plane epitaxial wafers can only work at low current densities as the current density increases due to the substantial decrease in efficiency. A better way to reduce this is to address the origin of the crystal plane's polarization field, so growing LED devices on semipolar planes is a well-known approach to droop reduction [10, 11]. Colloidal quantum dots (QDs) is suitable to use as a color conversion layer for  $\mu$ -LEDs, and a high contrast ratio can be achieved with QD-based  $\mu$ -LED displays [12, 13].

## 2. Results and Discussions

Fig. 1(a) represents the fluorescence microscopy (FLOM) image of RGB pixel matrices on glass showing a high contrast ratio between the gray PR matrices and the color pixels. Fig. 1(b) represents the EL spectra of semipolar blue  $\mu$ -LED, green and red pixels showing peak wavelengths of 453 nm, 536 nm and 630 nm respectively. The corresponding FWHM for the RGB emission spectra are 30.5 nm, 24.5 nm and 24.8 nm, hence these narrow FWHMs specify good performance in color rendering. It is clear that the blue light leakage has been reduced by using QDPR and it can be further reduced by increasing the thickness of QDPR or changing its composition. Since blue light leakage is minimized, only blue light from QD pixel remains, and each pixel will independently show brilliant colors. Hence, red and green QDPR pixels can filter blue light and significantly enhance the color purity.

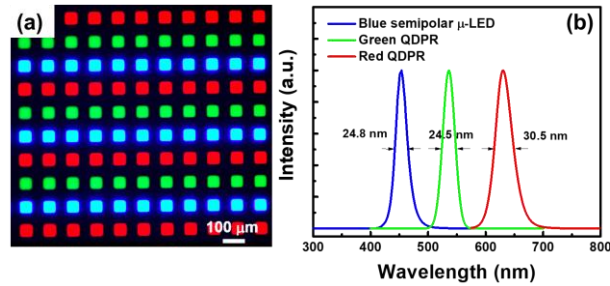


Fig. 1. (a) Fluorescence microscopy image of RGB pixel. (b) EL spectrum for blue  $\mu$ -LED, green and red pixel.

The color performance of the RGB  $\mu$ -LEDs under the injection current density from 1 A/cm<sup>2</sup> up to 200 A/cm<sup>2</sup> is demonstrated in Fig. 3 using CIE 1976. The color coordinates for c-plane device vary from (0.1572, 0.1067) to (0.1483, 0.0379) and for semi-polar device, the variation is from (0.1433, 0.0388) to (0.1490, 0.0317) in CIE 1931 chromaticity diagram. It is found that the color shift ( $\mu'v'$ ) for semipolar blue  $\mu$ -LEDs i.e. 0.0209 is smaller than that of c-plane which is 0.1374 in CIE 1976. The color gamut of the RGB made from semipolar  $\mu$ -LED is almost unchanged when the current density of the injection increases, although there is a variation of about 10% under the same conditions for c-plane device. Also, the red and green pixels display no color shift due to emission by optical pumping and stability of QDPR. The RGB pixel fabricated using semipolar  $\mu$ -LED and QDPR shows a wide-color gamut by achieving 114.4% of National Television Standards Committee (NTSC) space and 85.4% Rec. 2020 in the CIE 1931. Hence, the RGB pixels produced using semipolar  $\mu$ -LED and QDPR show excellent color stability and wide color gamut characteristics responsible for next generation display applications.

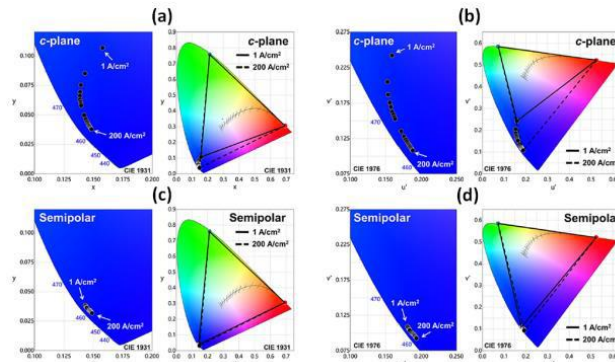


Fig. 2 (a) CIE 1931 and (b) CIE 1976 diagram for c-plane  $\mu$ -LED and QDPR. (c) CIE 1931 and (d) CIE 1976 diagram for semipolar  $\mu$ -LED and QDPR.

Fig. 3(a) is the electroluminescence (EL) microscope image of 3-in-1 RGB pixel. Fig. 2(b) and (c) presents a comparison of the PLQY of samples of RQDs and GQDs on BM under different pumping conditions. This finding indicates that the Al<sub>2</sub>O<sub>3</sub> layer minimizes the degradation caused by thermal and oxidative effects and effectively stabilizes the performance of QDs.

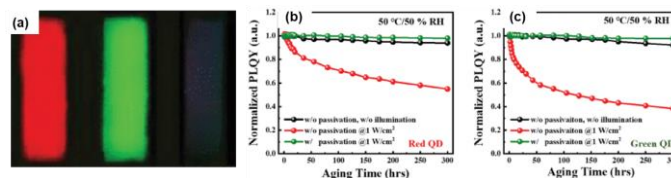


Fig. 3 (a) Fluorescence microscopy image of 3-in-1 RGB pixels. PLQY of (b) RQDs and (c) GQDs on black matrices under different excitation conditions.

The color performance of RGB mini-LEDs with and without ALD passivation after the 0–300 h lifetime test in the International Commission on Illumination-1976 (Commission Internationale de l'éclairage) (CIE-1976) is shown in Fig 4. The color coordinates in the sample with no ALD passivation varied from (0.5109, 0.5239) to (0.4092, 0.5353) and (0.0451, 0.5814) to (0.0521, 0.5793) in the CIE-1976 chromaticity diagram. The color shift ( $\Delta u'$ ,  $\Delta v'$ ) was (0.1017, 0.0114) for red color pixels and (0.0070, 0.0021) for green pixels in the CIE-1976. Moreover, the color coordinates for the treatment sample with ALD passivation varied from (0.5076, 0.5238) to (0.5054, 0.5241) and from (0.0442, 0.5813) to (0.0467, 0.5815), and the color shifts ( $\Delta u'$ ,  $\Delta v'$ ) were (0.0022, 0.0003) and (0.0025, 0.0002) in the CIE-1976, respectively, as shown in Fig. 4(b).

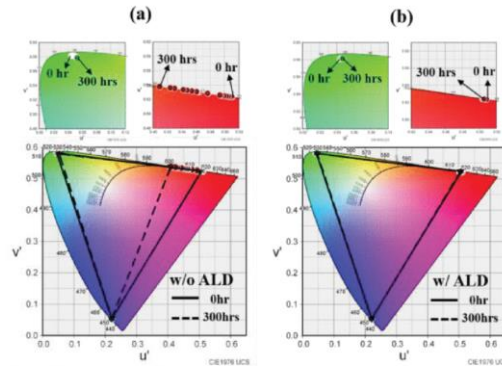


Fig. 4 Color gamut of RGB pixel assembly from (a) without ALD passivation, (b) with ALD passivation at different aging times in the CIE-1976.

Fig. 5 shows the hybrid quantum dot nanoring micro LEDs (QD-NR- $\mu$ LEDs) fabricated through electron beam (E-beam) lithography and QD printing. To create the color conversion layer, CdSe/ZnS red QDs were sprayed on a region of blue NR- $\mu$ LED through the super-inkjet (SIJ) printing system. The obtained NRET efficiency values of the QD-NR- $\mu$ LED with and without ALD passivation were 66.4% and 53.6%, respectively.

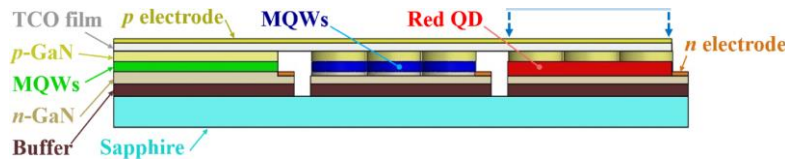


Fig. 5 Full-color monolithic hybrid quantum dot nanoring micro light-emitting diodes.

A schematic diagram of the *c*-plane InGaN red micro-LED epitaxial structure is demonstrated in Fig. 6. The fast carrier dynamics in the InGaN is characterized by using time-resolved photoluminescence, which is correlated to a high modulation bandwidth of 271 MHz achieved by a  $6 \times 25$ - $\mu\text{m}$ -sized micro-LED array with a data transmission rate of 350 Mbit/s at a high injection current density of 2000 A/cm<sup>2</sup>. The 100- $\mu\text{m}$ -sized device showed a lower bandwidth than 25- $\mu\text{m}$ -, 50- $\mu\text{m}$ -, and 75- $\mu\text{m}$ -sized ones at low current densities due to the current crowding effect and the limitation of the resistance capacitance (RC) time constant, but all of them are almost proportional to the current density. The NRZ-OOK eye diagrams are detected at 200 Mbit/s, 300 Mbit/s, and 390 Mbit/s, respectively. There is a clear and open eye diagram at 200 Mbit/s. At 300 Mbit/s, the eye is beginning to close, and is virtually closed at 390 Mbit/s. This shows the potential application of these micro-LEDs at data rates of the order of 300 Mbit/s.

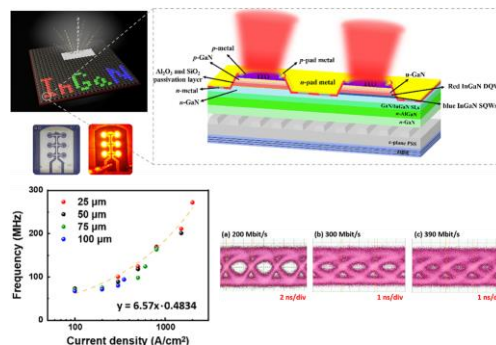


Fig. 6. Schematic diagram of *c*-plane InGaN red micro-LED epitaxial structure; frequency versus current density for different chip sized micro-LEDs; eye diagrams.

Fig. 7 illustrates a photograph of  $\mu$ LED operating at 10 mA and the 3 dB bandwidth increased with the current density because of the built-in electric field screening and decreased carrier lifetime due to the higher injected carrier density in the active region. As a result, the highest 3-dB bandwidth, which is up to 756 MHz, was realized by an injected current of 40 mA. These results suggest a good transmission capacity of green semipolar (20–21)  $\mu$ LEDs in VLC applications. Due to the impressive performance of the 3-dB bandwidth, the eye diagrams of the semipolar  $\mu$ LED were clear and open at both 1.0 and 1.5 Gb/s.

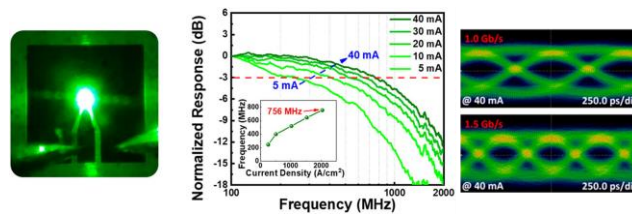


Fig. 6. An image of lighting from the device and the results for the frequency response measurement with eye diagram.

### 3. References

- [1] Liu, Zhitian, et al. "Efficient single-layer white light-emitting devices based on silole-containing polymers." *Journal of Display Technology* 9.6 (2013): 490-496.
- [2] Gong, Z., et al. "Efficient flip-chip InGaN micro-pixelated light-emitting diode arrays: promising candidates for micro-displays and colour conversion." *Journal of Physics D: Applied Physics* 41.9 (2008): 094002.
- [3] Wu, Tingzhu, et al. "Mini-LED and micro-LED: promising candidates for the next generation display technology." *Applied Sciences* 8.9 (2018): 1557.
- [4] Tan, Guanjun, et al. "High dynamic range liquid crystal displays with a mini-LED backlight." *Optics Express* 26.13 (2018): 16572-16584.
- [5] Cok, Ronald S., et al. "Inorganic light-emitting diode displays using micro-transfer printing." *Journal of the Society for Information Display* 25.10 (2017): 589-609.
- [6] K. J. Singh et al., "CsPbBr<sub>3</sub> perovskite quantum-dot paper exhibiting a highest 3 dB bandwidth and realizing a flexible white-light system for visible-light communication," *Photon. Res.* 9, 2341–2350 (2021).
- [7] Y.-M. Huang et al. "Gateway towards recent developments in quantum dot-based light-emitting diodes," *Nanoscale* 14, 4042–4064 (2022).
- [8] Takeuchi, Tetsuya, et al. "Quantum-confined Stark effect due to piezoelectric fields in GaInN strained quantum wells." *Japanese Journal of Applied Physics* 36.4A (1997): L382.
- [9] Takeuchi, Tetsuya, et al. "Determination of piezoelectric fields in strained GaInN quantum wells using the quantum-confined Stark effect." *Applied Physics Letters* 73.12 (1998): 1691-1693.
- [10] Feezell, Daniel F., et al. "Semipolar (20-2-1) InGaN/GaN light-emitting diodes for high-efficiency solid-state lighting." *Journal of Display Technology* 9.4 (2013): 190-198.
- [11] Masui, Hisashi, et al. "Nonpolar and semipolar III-nitride light-emitting diodes: Achievements and challenges." *IEEE Transactions on Electron Devices* 57.1 (2009): 88-100.
- [12] Achermann, Marc, et al. "Nanocrystal-based light emitting diodes utilizing high-efficiency nonradiative energy transfer for color conversion." *Nano Letters* 6.7 (2006): 1396-1400.
- [13] Erdem, Talha, and Hilmi Volkan Demir. "Color science of nanocrystal quantum dots for lighting and displays." *Nanophotonics* 2.1 (2013): 57-81.